Melt Fracture Behavior of Polypropylene-Type Resins with Narrow Molecular Weight Distribution. I. Temperature Dependence

MITSUYOSHI FUJIYAMA, HITOSHI INATA

Tokuyama Research Laboratory, Tokuyama Corp., 1-1, Harumi-cho, Tokuyama-shi, Yamaguchi-ken, 745-0024, Japan

Received 16 January 2001; accepted 26 July 2001

ABSTRACT: Polypropylene (PP)-type resins with narrow molecular weight distribution, such as PP-type thermoplastic elastomer PER and controlled-rheology PP (CRPP) made by peroxide degradation of high molecular weight PP, have a problem of easy generation of skin roughness at extrusion. To examine the present state, the occurrence of skin roughness in PER and CRPP at extrusion was investigated with a capillary rheometer in a shear rate range of 12–6100 s^{-1} and a temperature range of 180–280°C. A *homo*-PP (HPP) and a *block*-PP (BPP) with usual molecular weight distributions were used for comparison. HPP and BPP with usual molecular weight distributions show smooth extrudates at low shear rates and abruptly generate severe skin roughness "elastic failure" originating at the die entrance at a higher shear rate. PER and CRPP with narrow molecular weight distributions easily generate "sharkskin" melt fracture originating at the die exit, from a shear rate nearly one decade lower than rates of elastic failure of HPP and BPP. The sharkskin becomes more severe, with increasing shear rate, and attains to the elastic failure. The critical shear rate at which sharkskin occurs increases with increasing extrusion temperature. The critical shear rate is about 20 s^{-1} at 180°C and about 120 s^{-1} at 280°C, which is in the range encountered by the molten resin at extrusion processing. © 2002 Wiley Periodicals, Inc. J Appl Polym Sci 84: 2111–2119, 2002

Key words: polypropylene-type resins; extrusion; sharkskin; elastic failure; critical shear rate

INTRODUCTION

Polypropylene (PP)-type thermoplastic elastomer P.E.R. (PER, produced by Tokuyama Corp., Japan) is a reactor-type thermoplastic elastomer and is used in fields of injection molding and film/sheet extrusions.[1–3] PER has a problem of easy generation of sharkskin melt fracture at extrusion and is expected to suppress it, given that PER has a narrow molecular weight distribution compared to that of usual PP. The controlled-rheology PP made by peroxide degradation of high molecular weight PP also has a narrow molecular weight distribution and hence possesses the same problem.

Various types of skin roughness occur at polymer melt extrusion: scratches, sharkskin, bambooing, spiraling, irregular fracture, and so forth. The sharkskin and irregular fracture frequently appear. PER and CRPP also generate these two types of skin roughness as shown later.

Two types of theories are proposed for the mechanism of "sharkskin." One is based on the

Correspondence to: M. Fujiyama (m-fujiyama@tokuyama.co.jp).

Journal of Applied Polymer Science, Vol. 84, 2111–2119 (2002)

Table I Characteristics of Samples

Sample Code	PER	CRPP	HPP	BPP
Grade	T310E	KPP-1	YD121	MS624
Ethylene content (wt %)	22.4	0	0.5	4.0
M_n	119,000	111,000	65,800	66,700
M_w	244,000	342,000	461,000	441,000
M_w/M_n	2.1	3.1	7.0	6.6
MFI (g/10 min)	1.77	1.71	1.75	1.70
Die swell ratio	1.40	1.11	1.26	1.16

stick-slip at the die wall[4–10] and the other is based on the periodic growth and relaxation of tensile stress at the extrudate surface at the die exit.[11–20] The sharkskin is considered to occur at a constant extrudate velocity and its critical velocity increases with increasing temperature.[11,12,21,22] It occurs at a lower shear rate for a resin with narrower molecular weight distribution.[8,12,22–24] Although molecular weight does not influence the sharkskin as much as its distribution does, a resin with higher molecular weight more easily generates the sharkskin.[22,23] Recently, a trial of explaining the sharkskin on a molecular basis was proposed. Wang et al.[25,26] proposed an "interfacial molecular instability mechanism," which states that the sharkskin occurs because of a local conformational transition at the die exit wall where the absorbed chains trap a layer of interfacial chains. This layer oscillates between entanglement and disentanglement states attributed to a reversible coil–stretch transition. The sharkskin generally occurs from lower shear rate or stress than those from elastic failure mentioned below. These experimental facts were obtained mainly for high-density polyethylene, linear low-density polyethylene, and polydimethylsiloxane, with relatively narrow molecular weight distributions.

The irregular fracture, on the other hand, is a phenomenon in which stored elastic energy at the die entrance cannot be held anymore and released at the die exit, called "elastic failure".[11,27] The critical shear rate and stress of the elastic failure are the higher as the molecular weight is the lower and the extrusion temperature is the higher and the dependency of the critical shear stress on the molecular weight and temperature is by far less than that of the critical shear rate.[11,28] The elastic failure occurs from lower shear rate as the molecular weight distribution is broader.[24]

To examine the present state of melt fracture behaviors of PER and CRPP, they were extruded with a capillary rheometer at an extrusion temperature interval of 20°C in a temperature range of 180–280°C and the extrudates were observed. Furthermore, to clarify the mechanism of sharkskin of PP-type resins with narrow molecular weight distributions such as PER and CRPP, capillary extrusion experiments were carried out by using three dies with the same capillary length (L)/diameter (D) ratio and different D values and by using three dies with the same D and different L values. A *homo*-PP (HPP) and a *block*-PP (BPP) with the usual molecular weight distributions and similar melt flow indices (MFIs) to those of PER and CRPP were used for comparison.

EXPERIMENTAL

Samples

Table I shows characteristics of the samples used. PER used was P.E.R. T310E (M_w/M_n = 2.1) manufactured by Tokuyama Corp. (Japan). CRPP (M_w/M_n = 3.1) was made by peroxide degradation of an ultrahigh molecular weight PP with a screw extruder. HPP and BPP used were Tokuyama Polypro YD121 (M_w/M_n = 7.0) and MS624 (M_w/M_n = 6.6) manufactured by Tokuyama Corp., respectively. Because PER is a kind of propylene/ethylene block copolymer with high content of EPR copolymer portion,[1–3] it is preferably compared with BPP. Meanwhile, because CRPP is a degraded *homo*-PP, it is preferably compared with HPP.

Extrusion Test with Melt Indexer

To characterize the samples, melt flow index, flow activation energy, and die swell ratio were measured with a melt indexer (X416 Type; Takara Thermistor Instruments Co. Ltd., Japan) under 2160 g load at 200, 230, and 260°C.

Table II Dimensions of Dies

NO	Length L (mm)	Diameter D (mm)	L/D
1	5.0	0.5	10
2	10.0	1.0	10
3	20.0	2.0	10
4	5.0	1.0	5
5	20.0	1.0	20

Extrusion Test with Capillary Rehometer

Capillary flow properties were measured with a capillary rheometer (Capirograph 1B Type; Toyo Measurement Instruments Co. Ltd., Japan). The dimensions of stainless steel dies used are shown in Table II.

For all samples in Table I, the flow curves were measured with no. 2 die (L = 10 mm; D = 1 mm; L/D = 10) at an extrusion temperature interval of 20°C at a temperature range of 180–280°C under extrusion speeds of 1–500 mm/min, and the extrudate surfaces were observed with a magnifier.

For PER and CRPP, extrusion tests were carried out by use of three dies (1, 2, and 3) with the same L/D (=10) and different D values, and the slip velocities at the die wall were evaluated by the Mooney method.[29] At the same time, whether the sharkskin occurs at a constant extrusion velocity or at a constant shear rate was examined.

The influence of capillary length L on the melt fracture behavior of PER was examined by use of three dies (2, 4, and 5) with the same D (=1 mm) and different values of L.

The apparent shear rate at the die wall $\dot{\gamma}_w$, apparent shear stress τ_w, and apparent shear viscosity η_a are given by eqs. (1), (2), and (3), respectively:

$$\dot{\gamma}_w = \frac{4Q}{\pi R^3} \tag{1}$$

$$\tau_w = \frac{PR}{2L} \tag{2}$$

$$\eta_a = \frac{\tau_w}{\dot{\gamma}_w} \tag{3}$$

where L (cm) is the capillary length, D (=2R) (cm) is the capillary diameter, Q (cm^3/s) is the volumetric extrusion rate, and P (Pa) is the extrusion pressure.

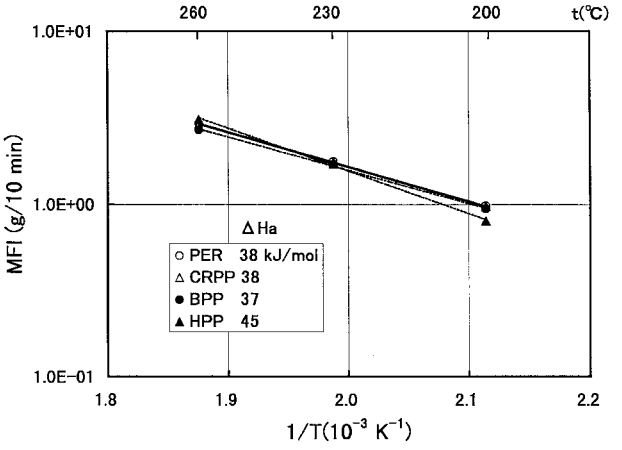

Figure 1 Temperature dependence (Arrhenius plot) of melt flow index (MFI).

Observation of Extrudate

Optical micrographs of PER extrudates extruded with a die of L = 10 mm, D = 1 mm, and L/D = 10 at 240°C were taken under a magnification of ×30.

RESULTS AND DISCUSSION

Characterization of Samples

Figure 1 shows the temperature change (Arrhenius plot) of MFI. Although the activation energy ΔH_a of HPP is 45 kJ/mol and a little higher than that of the others (37–38 kJ/mol and nearly the same), it may be regarded that the temperature dependency of viscosity of PER is nearly the same as that of PP.

Figure 2 shows the temperature change of die swell ratio D/D_0. Given CRPP's narrow molecular

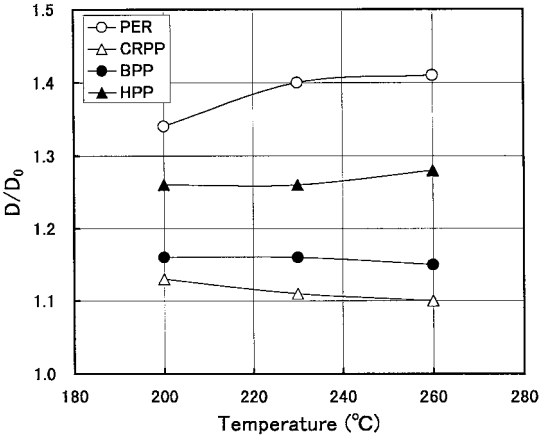

Figure 2 Temperature dependence of die swell ratio D/D_0.

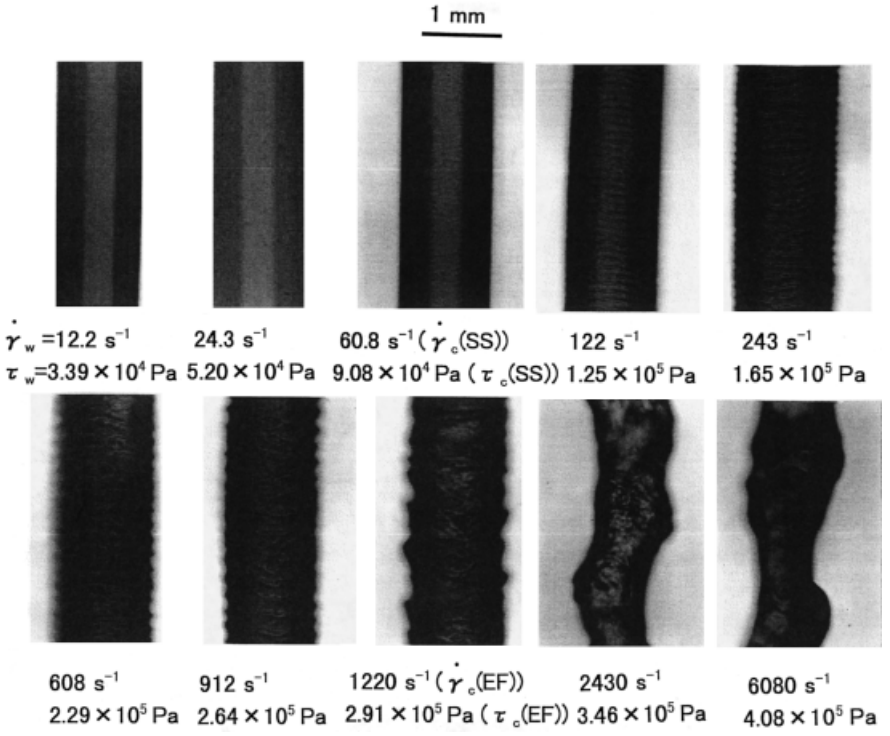

Figure 3 Optical micrographs of PER extrudates. 240°C, Die: L = 10 mm, D = 1 mm, L/D = 10.

weight distribution, its die swell ratio is smaller than that of HPP. In spite of narrow molecular weight distribution, PER shows large die swell ratio because PER is a blend of PP and EPR and shows a multiphase network structure.[3]

Melt Fracture Behavior

Figure 3 exemplifies optical micrographs of PER extrudates extruded at various extrusion speeds at 240°C by use of a die with L = 10 mm, D = 1 mm, and L/D = 10. The extrudates are smooth at shear rates of 12.2 s^{-1} and 24.3 s^{-1}, a weak sharkskin appears at 60.8 s^{-1}, grows gradually with increasing shear rate, and attains to an elastic failure at 1220 s^{-1}. Accordingly, for this sample under these extrusion conditions, the critical shear rate at which a sharkskin begins to occur, $\dot{\gamma}_c$(SS), is 60.8 s^{-1} and the critical shear stress τ_c(SS) is 9.08 $\times$ 10^4/Pa. Similarly, the critical shear rate for elastic failure $\dot{\gamma}_c$(EF) is 1220 s^{-1} and the critical shear stress τ_c(EF) is 2.91 $\times$ 10^5 Pa. It can be said that the higher the value of $\dot{\gamma}_c$(SS), the wider the extrusion speed range where fine extrudates can be obtained.

Figure 4 shows the temperature changes of $\dot{\gamma}_c$(SS), $\dot{\gamma}_c$(EF), τ_c(SS), and τ_c(EF). As shown in Figure 4(a), for PER $\dot{\gamma}_c$(SS) increases with increasing extrusion temperature and is about 20 s^{-1} at 180°C and about 120 s^{-1} at 280°C, which is in the shear rate range that a molten resin encounters at extrusion processing. $\dot{\gamma}_c$(EF) also increases with increasing extrusion temperature at a slope similar to that of $\dot{\gamma}_c$(SS) and is about 400 s^{-1} at 180°C and about 4000 s^{-1} at 280°C. τ_c(SS) and τ_c(EF) are independent of extrusion temperature and are 1 $\times$ 10^5 Pa and 3 $\times$ 10^5 Pa, respectively. Other grades of PER also show similar melt fracture behaviors to those of this grade. The experimental results for temperature dependency of $\dot{\gamma}_c$(SS) of PER show similar tendencies to those of HDPE by Howells and Benbow,[11] by Clegg,[21] and by Staubler et al.[22] Furthermore, it has been shown that the value of τ_c(SS) is 1–3 $\times$ 10^5 Pa, independent of the kind of polymer and extrusion temperature, agreeing with the present value of PER.

Figure 4(b) shows the results of CRPP. CRPP, like PER, also shows a sharkskin. This is assumed to be because of its narrow molecular weight distribution. As stated in introductory remarks, the sharkskin easily occurs when the molecular weight distribution is narrow. Given that the sharkskin also occurs for *homo*-PP with a narrow molecular weight distribution like that of

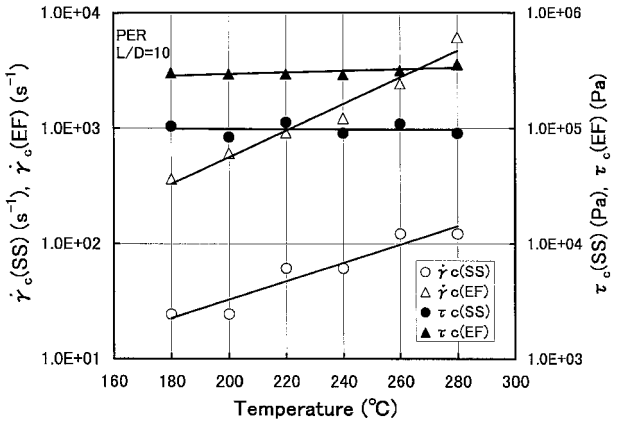

(a)

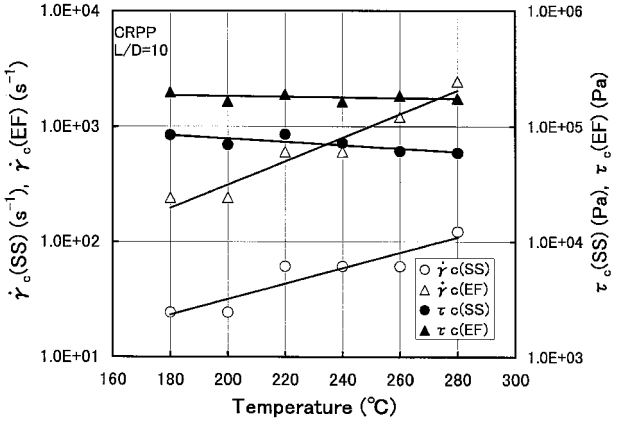

(b)

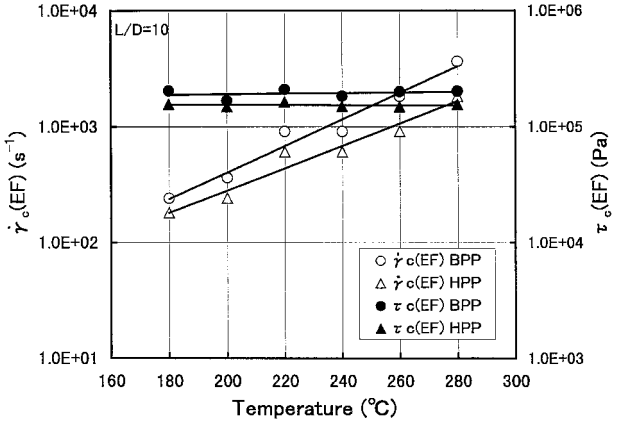

(c)

Figure 4 Temperature changes of critical shear rate at which sharkskin begins to occur, $\dot{\gamma}_c$(SS), critical shear stress τ_c(SS), critical shear rate at which elastic failure begins to occur, $\dot{\gamma}_c$(EF), and critical shear stress τ_c(EF). (a) PER, (b) CRPP, (c) BPP and HPP.

CRPP, it is assumed that the cause of sharkskin of PER arises from its narrow molecular weight distribution. $\dot{\gamma}_c$(SS) and $\dot{\gamma}_c$(EF) of CRPP are nearly the same as those of PER, whereas τ_c(SS) and τ_c(EF) of CRPP are slightly higher than those of PER and nearly the same as those of BPP and HPP.

Figure 4(c) shows the results of BPP and HPP. These PPs do not generate the sharkskin and abruptly generate an elastic failure when the extrusion speed is increased. $\dot{\gamma}_c$(EF) and τ_c(EF) of these PPs are considerably lower than those of PER.

Effect of Capillary Diameter on Melt Fracture Behavior

The effects of capillary diameter D on the critical shear rate and critical shear stress is shown in Figure 5(a) for PER and in Figure 5(b) for HPP. These figures show that the melt fracture behavior is scarcely affected by D.

If the melt fracture occurs at a constant extrusion velocity, $\dot{\gamma}_c \times D$ must be constant.[14] However, the experimental results show that it is not the case, although $\dot{\gamma}_c$ is constant. Accordingly, it may be said that both the sharkskin and the elastic failure begin to occur at a constant shear rate or stress.

As mentioned in the introductory remarks, a cause of the sharkskin is considered to be a slip at the die wall. If a slip at the die wall exists, the following Mooney equation[29] holds with v_0 for the slip velocity:

$$\dot{\gamma}_w = \frac{4Q}{\pi R^3} = 4v_0\frac{1}{R} + \frac{4}{\tau_w^4}\int_0^{\tau_w} \tau^2 f(\tau)d\tau \qquad (4)$$

Accordingly, apparent flow curves are first measured by use of dies with the same L/D and different values of D (=$2R$) and then $\dot{\gamma}_w = 4Q/\pi R^3$ at constant τ_w is plotted against $1/R$ for each τ_w, which gives linear relationships. The slip velocity v_0 is obtained from the slope.

Representative apparent flow curves at 200°C, 240°C, and 280°C are shown in Figure 6(a)–(c) for PER and in Figure 7(a)–(c) for HPP. It is seen from Figures 6 and 7 that for both PER and HPP the influence of D is more remarkable at lower temperatures, which means that the slip occurs more easily at lower temperatures. From the fact that the slip is observed for HPP even as it is for PER, the sharkskin of PER cannot be explained only by the slip at the die wall.

Effect of Capillary Length on Melt Fracture Behavior

Figure 8 shows the effect of capillary length L on the melt fracture behavior of PER as an example.

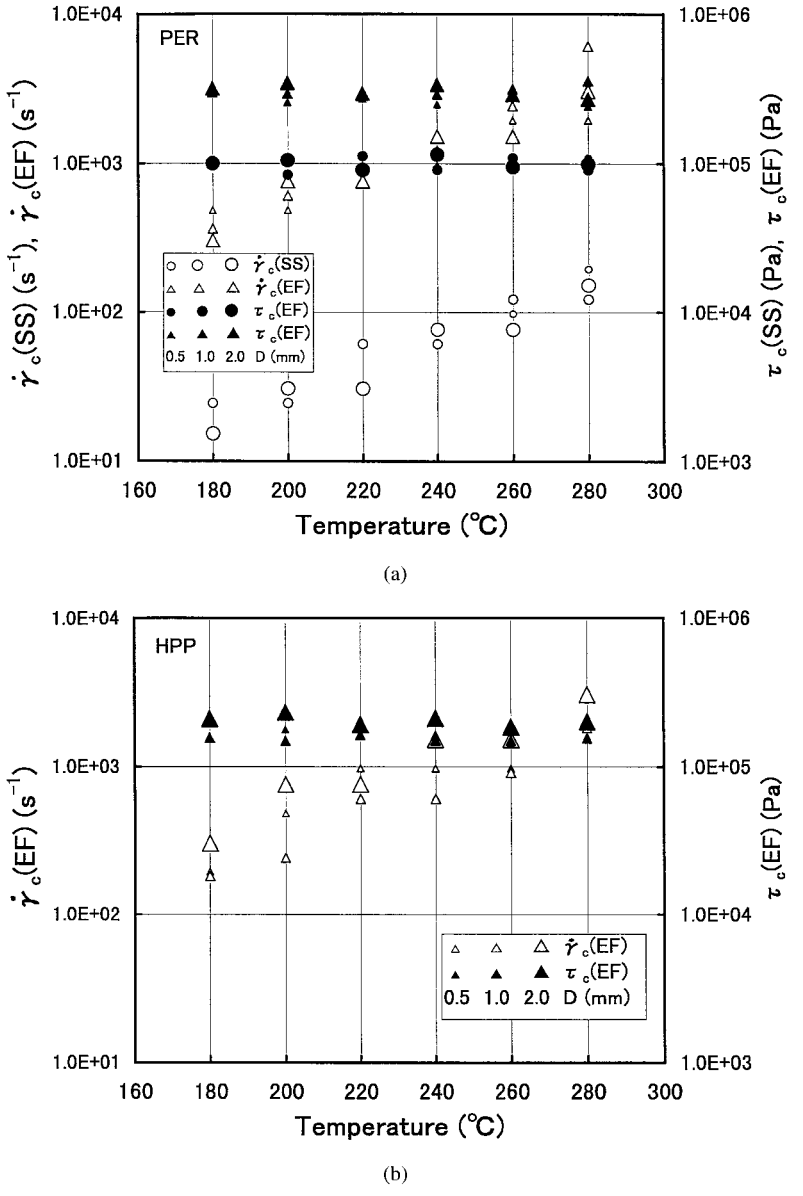

Figure 5 Dependency of critical shear rate and critical shear stress on capillary diameter D. $L/D = 10$: (a) PER, (b) HPP.

Although $\dot{\gamma}_c$(SS) and τ_c(SS) are scarcely affected by L, $\dot{\gamma}_c$(EF) and τ_c(EF) are higher as L becomes shorter. This is assumed to be because an apparent shear stress without end correction is used as the shear stress and, hence, the shear stress measured with the shorter die is calculated apparently the higher. That the effect of L is scarcely observed for sharkskin, whereas it appears remarkably for elastic failure, is assumed to be partly because the former begins to occur at a low shear rate where the end correction term is small.

Moynihan et al.[14] studied the effect of L on the sharkskin of LLDPE and found that long L suppressed the sharkskin. They concluded that the die entry region plays an important role and a longer die damps the fracture generated at the entry region more than it does at the die land region. L scarcely affected the sharkskin in the present experiments for PP-type resins, not agreeing with that of Moynihan et al.,[14] whose reason is not clear at the present time.

CONCLUSIONS

Polypropylene (PP)-type resins with narrow molecular weight distribution, such as PER and

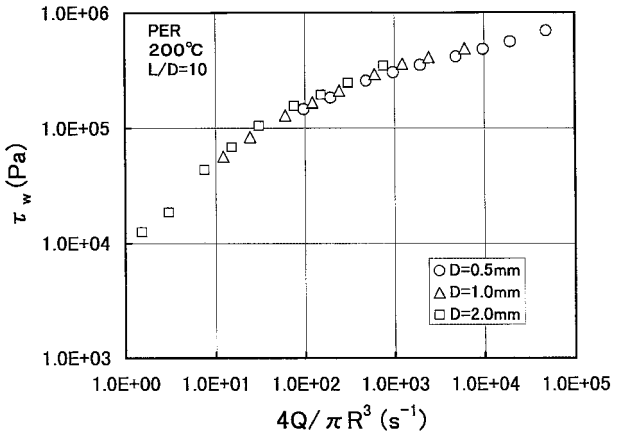

(a)

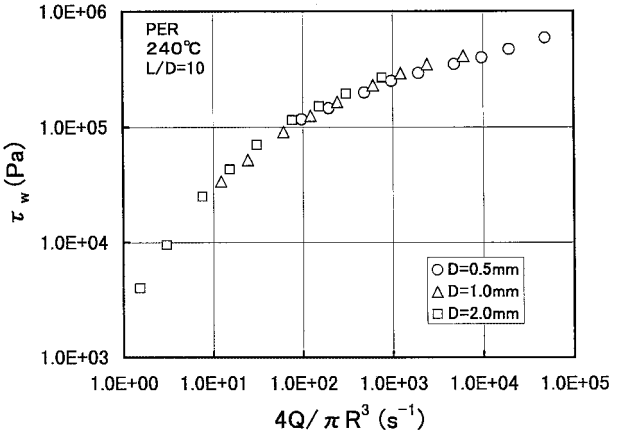

(b)

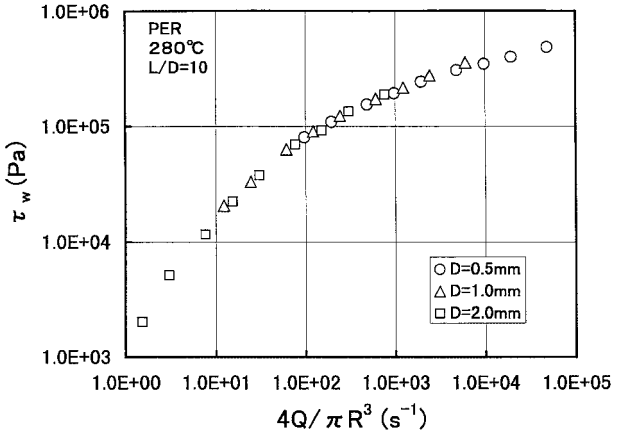

(c)

Figure 6 Flow curves measured by use of three dies with same *L/D* (=10) and different *D* values (Mooney plots). PER: (a) 200°C, (b) 240°C, (c) 280°C.

CRPP, have a problem of easy generation of skin roughness at extrusion. To examine the present state, the occurrence of skin roughness in PER and CRPP at extrusion was investigated with a capillary rheometer in a shear rate range of 12–6100 s^{-1} and a temperature range of 180–280°C. HPP and BPP with the usual molecular weight

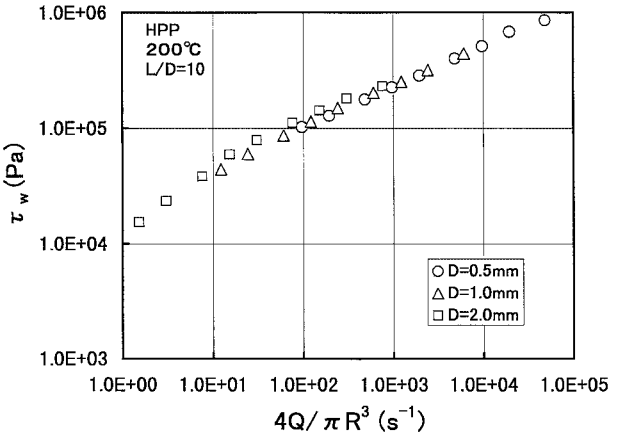

(a)

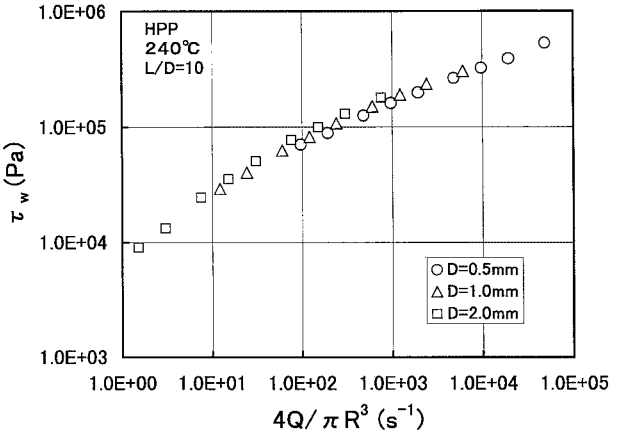

(b)

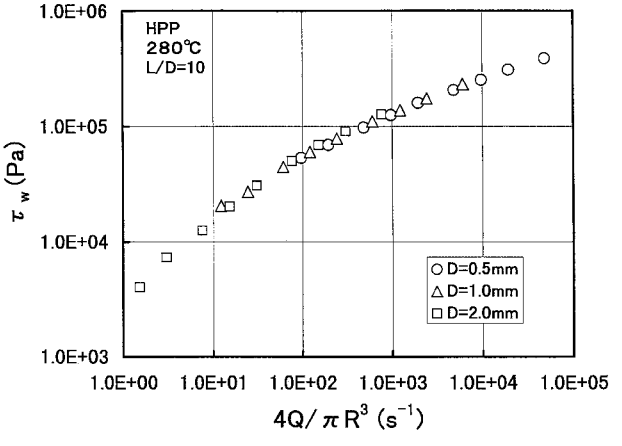

(c)

Figure 7 Flow curves measured by use of three dies with same *L/D* (=10) and different *D* values (Mooney plots). HPP: (a) 200°C, (b) 240°C, (c) 280°C.

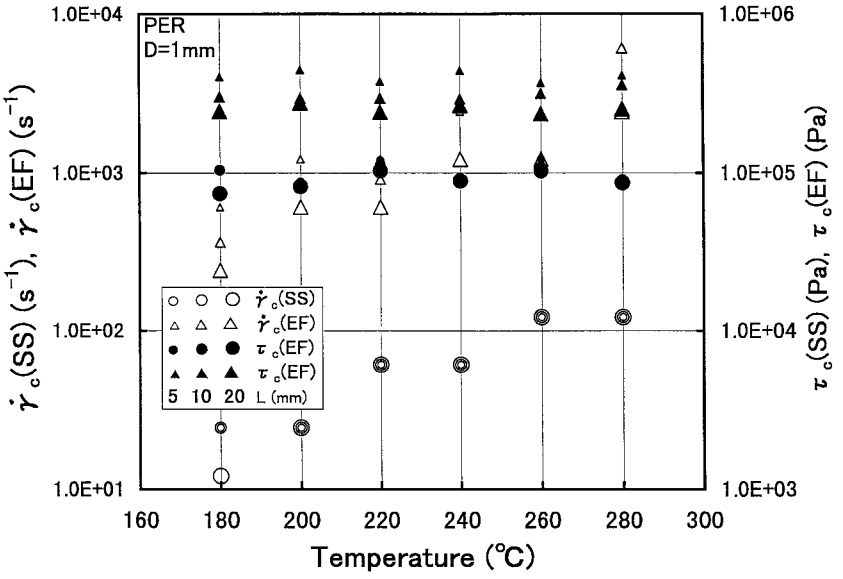

Figure 8 Dependency of critical shear rate and critical shear stress on capillary length L. PER: D = 1 mm.

distributions were used for comparison. The following results were obtained:

1. HPP and BPP show smooth extrudates at low shear rates and abruptly generate severe skin roughness "elastic failure" originating at the die entrance at a higher shear rate. PER and CRPP easily generate "sharkskin" melt fracture originating at the die exit, from a shear rate nearly one decade lower than rates of elastic failure of HPP and BPP. The sharkskin becomes more severe, with increasing shear rate, and attains to the elastic failure. The critical shear rate at which sharkskin occurs increases with increasing extrusion temperature.
2. Melt fractures such as sharkskin and elastic failure are scarcely affected by capillary diameter and, hence, do not occur at a constant extrusion velocity but at a constant shear rate or stress.
3. Although the slip of resin at the die wall is more remarkable at lower extrusion temperatures, the slip of PER does not differ very much from that of HPP. Accordingly, the occurrence of sharkskin cannot be explained only by the slip.
4. The critical shear rate and stress at which the elastic failure begins to occur are lower as the capillary length is longer, whereas those of the sharkskin scarcely depend on it.

The melt fracture behaviors of PP-type resins with narrow molecular weight distribution generally agree with the previous information obtained mainly for LLDPE, with some exceptions. The mechanism of sharkskin of PP-type resins cannot be presumed only from the present investigation and further study is needed, which will be reported in a following study.

The authors thank Tokuyama Corp. for permission to publish this study.

REFERENCES

1. Ogata, T. Jpn Plast 1993, 44(11), 88.
2. Yamamoto, Y.; Nakanishi, H. Convertech 1994, 22(7), 2.
3. Yamamoto, Y. in Proceedings of the 8th Polymer ABC Research Meeting, Tokyo, Japan, 1995; p 3.
4. Ramamurthy, A. V. J Rheol 1986, 30, 337.
5. Kalika, D. S.; Denn, M. M. J Rheol 1987, 31, 815.
6. Iwakura, K.; Abe, Y.; Takita, M.; Masuko, T.; Kobayashi, H. Seikei-Kakou (Journal of the Japan Society of Polymer Processing) 1989, 1, 220.
7. Kissi, N. E.; Piau, J. M. J Non-Newtonian Fluid Mech 1990, 37, 55.
8. Kendal, V. G. Trans J Plast Inst 1963, 31, 49.
9. Hatzikiriakos, S. G.; Hong, P.; Ho, W.; Stewart, C. W. J Appl Polym Sci 1995, 55, 595.
10. Ghanta, V. G.; Riise, B. L.; Denn, M. M. J Rheol 1999, 43, 435.
11. Howells, E. R.; Benbow, J. J. Trans J Plast Inst 1962, 30, 240.

12. Cogswell, F. N. J Non-Newtonian Fluid Mech 1977, 2, 37.
13. Piau, J. M.; Kissi, N. E.; Tremblay, B. J Non-Newtonian Fluid Mech 1990, 34, 145.
14. Moynihan, R. H.; Baird, D. G.; Ramanathan, R. J Non-Newtonian Fluid Mech 1990, 36, 255.
15. Tremblay, B. J Rheol 1991, 35, 985.
16. Kissi, N. E.; Piau, J. M. J Rheol 1994, 38, 1447.
17. Kurtz, S. J. Proceeding of 10th Meeting of the Polymer Processing Society (PPS), 1994, p 8.
18. Baird, D. G.; Tong, P. P. SPE Technical Papers, 53rd ANTEC 1995, 41, 1095.
19. Kissi, N. E.; Piau, J. M.; Toussaint, F. J Non-Newtonian Fluid Mech 1997, 68, 271.
20. Inn, Y. W.; Fischer, R. J.; Shaw, M. T. Rheol Acta 1998, 37, 573.
21. Clegg, P. L. Trans J Plast Inst 1960, 28, 245.
22. Stabler, H. G.; Haward, R. N.; Wright, B. Advances in Polymer Science and Technology, S.C.I. Monograph, No. 6, 1967; p 327.
23. Endo, H.; Kuroda, T. in Proceedings of 21st Rheology Meeting, Kyoto, Japan, 1973; p 114.
24. Goyal, S. K.; Kazatchkov, I. B.; Bohnet, N.; Hatzikiriakos, S. G. SPE Technical Papers; 55th ANTEC 1997, 43, 1076.
25. Wang, S. Q.; Drda, P. A.; Inn, Y. W. J Rheol 1995, 40, 875.
26. Barone, J. R.; Plucktaveesak, N.; Wang, S. Q. J Rheol 1998, 42, 813.
27. Tordella, J. P. Trans Soc Rheol 1957, 1, 203.
28. Spencer, R. S.; Dillon, R. E. J Colloid Sci 1949, 4, 251.
29. Mooney, M. J Rheol 1931, 2, 210.